

Regge models of the proton structure function with and without hard Pomeron: a comparative analysis

P. Desgrolard ^{a,1}, E. Martynov ^{b,2}

^a Institut de Physique Nucléaire de Lyon, IN2P3-CNRS et Université Claude Bernard, 43 boulevard du 11 novembre 1918, F-69622 Villeurbanne Cedex, France

^b Bogolyubov Institute for Theoretical Physics, National Academy of Sciences of Ukraine, 03143 Kiev-143, Metrologicheskaja 14b, Ukraine

Abstract A comparative phenomenological analysis of Regge models with and without a hard Pomeron component is performed using a common set of recently updated data. It is shown that the data at small x do not indicate explicitly the presence of the hard Pomeron. Moreover, the models with two soft-Pomeron components (simple and double poles in the angular momentum plane) with trajectories having intercept equal one lead to the best description of the data not only at $W > 3$ GeV and at small x but also at all $x \leq 0.75$ and $Q^2 \leq 30000$ GeV².

1 Introduction

It can be asserted confidently that Regge theory [1] is one of the most successful approaches to describe high energy scattering of hadrons. Since some of important ingredients of amplitudes such as vertex functions or couplings cannot be calculated (derived) theoretically, a number of models are based on additional assumptions. Concerning the leading Regge singularity, the Pomeron, even its intercept is a subject of lively discussions. Moreover, the proper Regge models as well as the models inspired by QCD or by other approaches, having elements of Regge approach, are more or less successful when applied to processes induced by photons (for an obviously incomplete list, see [2]-[16]).

Two methods are currently used to construct a phenomenological Pomeron model for pure hadronic amplitudes. In the first one, the Pomeron is supposed to be a simple pole in the angular momentum (j -) plane, with intercept $\alpha_P(0) > 1$. This property is necessary to explain the observed growth of the total cross-sections with energy. Then, such a Pomeron must be unitarized because it violates unitarity. In the second approach, the amplitude is

¹E-mail: desgrolard@ipnl.in2p3.fr

²E-mail: martynov@bitp.kiev.ua

constructed, from the start, in accordance with general requirements imposed by unitarity and analyticity. Here Pomeron has $\alpha_P(0) = 1$ and must be a singularity harder than the simple pole is (again because of the rising cross-sections).

The hypothesis of Pomeron with $\alpha_P(0) > 1$ (called sometimes "supercritical" Pomeron) has a long history (see for example [17]); it is supported presently by perturbative QCD where BFKL Pomeron [18] has $\Delta_P = \alpha_P(0) - 1 \approx 0.4$ in the leading logarithmic approximation (LLA). However, the next correction to Δ_P LLA is large and negative [19], the further corrections being unknown yet. As a consequence, the intercept of the Pomeron is usually determined phenomenologically from the experimental data. In their popular supercritical Pomeron model, Donnachie and Landshoff [20] found $\alpha_P(0) = 1.08$ from the data on hadron-hadron and photon-hadron total cross-sections. When the model was applied in deep inelastic scattering, namely to the proton structure functions, the authors needed to add a second Pomeron, "hard", (in contrast with the first one called "soft" Pomeron, because of its intercept near 1), with a larger intercept $\alpha_{hP}(0) \approx 1.4$ [7, 16].

At the same time, the detailed comparison [21]-[23] of various models of Pomeron with the data on total cross-section shows that a better description (less value of χ^2 and more stable values of fitted parameters when the minimal energy of the data set is varying) is achieved in alternative models with Pomeron having intercept one, but being a harder j -singularity, for example, a double pole. Thus, the Soft Dipole Pomeron (SDP) model was generalized for the virtual photon-proton amplitude and applied to the proton structure function (SF) in a wide kinematical region of deep inelastic scattering [8]. This model also has two Pomeron components, each of them with intercept $\alpha_P(0) = 1$, one is a double pole and the other one is a simple pole.

Recent measurements of the SF have become available, from H1 [24] and ZEUS [25] collaborations ; they complete or correct the previous data near the HERA collider [26]-[29] and [30]-[32] and from fixed target experiments [33]-[37]. They have motivated us to test and compare above mentioned Pomeron models of the proton structure function $F_2(x, Q^2)$ for the widest region of Q^2 and x .

In this paper, we would like to determine how is crucial or no the existence of a hard Pomeron component (having in mind the previous successes of the Soft Dipole Pomeron model without a hard Pomeron component). We support the point of view that Pomeron is an universal Reggeon: only the vertex functions are different with different processes. That means that the Pomeron trajectory (or trajectories in the case of two components) could not depend on the external particles *i.e.* on the virtuality Q^2 of photon in DIS. This circumstance dictates partially the choice of the models under consideration. Our aim is to propose a detailed quantitative comparison of some models, satisfying the hypothesis of universality, with and without a hard Pomeron.

Details on the fitting procedure, particularly on the choice of experimental data, are given in the next section. In Sect.3, the proposed models are defined (or redefined), their comparison is performed in two steps : the low x analysis allows to select the best ones kept in the extended x -range.

2 Fitting procedure : details

The choice of a data set may have crucial consequences in definitive conclusions of any analysis. Thus, a set including the most recent and older data has been used in the fits of the models of the proton SF. These updated data are listed and referenced in Table 1. We

have fitted the models in three kinematic regions: A, B and C.

$$W > 6 \text{ GeV}, \quad x \leq 0.07, \quad Q_{max}^2 = 3000 \text{ GeV}^2, \quad \text{Region A.} \quad (2.1)$$

$$W > 3 \text{ GeV}, \quad x \leq 0.07, \quad Q_{max}^2 = 3000 \text{ GeV}^2, \quad \text{Region B} \quad (2.2)$$

$$W > 3 \text{ GeV}, \quad x \leq 0.75, \quad Q_{max}^2 = 3000 \text{ GeV}^2, \quad \text{Region C} \quad (2.3)$$

The determination of the regions A (with 797 points) and B (with 878 points) is arbitrary enough, especially concerning the upper limit for x , aiming to select "small" x .

The second region (B) is the extension of region A for $W > 3 \text{ GeV}$. One can see from Table 1 that the difference between both comes mainly from the added data on the cross-section $\sigma_{tot}^{\gamma p}$, when we are going from A to B.

We remark that the pure hadronic cross-sections data at $\sqrt{s} \geq 5 \text{ GeV}$ are described well by the Dipole Pomeron [22, 23], whereas the physical threshold for NN interaction is $\sqrt{s_{NN}} \sim 2 \text{ GeV}$. For γN interaction the threshold is lower, $\sqrt{s_{\gamma N}} \equiv W_{\gamma N} \sim 1 \text{ GeV}$. Thus one can expect a good description of the low W -data at least within the Soft Dipole Pomeron model.

Table 1: Observables sets used in the fitting procedure (note that the mentioned year does not correspond to the data-taking period, but rather to the final publication. For description of the different regions, see the text.

Observable Exp. – year of pub.,	Ref	Region A(A ₁) Nb points	Region B(B ₁) Nb points	Region C Nb points
F_2^p				
H1 – 1995	[26]	85	85	93
H1 – 1996	[27]	37	37	41
H1 – 1997	[28]	21	21	21
H1 – 2000	[29]	51	51	111
H1 – 2001	[24]	127	127	133
ZEUS – 1996	[30]	153	153	186
ZEUS – 1997	[31]	34	34	34
ZEUS – 1999	[32]	44	44	44
ZEUS – 2000	[25]	70	70	70
NMC – 1997	[33]	59	65	156
E665 – 1996	[34]	80	80	91
SLAC – 1990/92	[35]	0	7(0)	136
BCDMS – 1989	[36]	5(0)	5(0)	175
$\sigma_{tot}^{\gamma,p}$				
1975/78; ZEUS – 1994; H1 – 1995	[37]	31	99	99
Total		797(792)	878(866)	1390

Running a few steps forward we should note that there are a few data points from the fixed target experiments [35], [36] in the above mentioned regions A (5 points of BCDMS experiment) and B (5 points of BCDMS and 7 points of SLAC experiments) that lead to some problems in the fit. Firstly, they contribute to the χ^2 noticeably more than the other points do. Secondly, an analysis of all the models we consider here shows that they destroy the stability of the parameters values when one goes from region A to region B. The problems disappear if these 12 points are eliminated from our fit. Possibly, at small x , there is a small

inconsistency (due to normalization ?) between the experiments. In the following, we present the detailed results of a fit without these points (the corresponding data sets are noted as A_1 and B_1), but we give also the values of χ^2 for the full data sets, A and B.

The third region (C) includes all data listed in Table 1. The relative normalization among all the experimental data sets has been fixed to 1. Following the suggestion from [29], some data from [27] are considered as obsolete and superseded. They correspond to ($Q^2 \geq 250$ GeV², for all x), ($Q^2 = 200$ GeV², for $x < 0.1$) and ($Q^2 = 150$ GeV², for $x < 0.01$). We also cancelled the ancient values (with moderate $Q^2 \leq 150$ GeV²: 88 from [27] and 23 from [28]) which have been duplicated in the more recent high precision measurements [24]. We have excluded the whole domain $Q^2 \geq 5000$ GeV² from the fit (19 data points from [29] and 2 from [30]), because the difference (experimentally observed) between e^-p and e^+p results cannot be (and should not be) explained by Pomeron + f exchange. No other filtering of the data has been performed. Experimental statistical and systematic errors are added in quadrature.

As usual, we "measure" the quality of agreement of each model with experimental data by the χ^2 , minimized using the MINUIT computer code. The ensuing determination of the free parameters is associated with the corresponding one-standard deviation errors. The results are displayed below ³.

3 Regge models in Deep Inelastic Scattering and phenomenological analysis

We stress again that there are numerous models for the proton SF, inspired by a Regge approach, which describe more or less successfully the available data on the SF in a wide region of Q^2 and x . Here, we consider two of them (and their modifications): the two-Pomeron model of Donnachie and Landshoff [7] and the Soft Dipole Pomeron model [8], incorporating explicitly the ideas of universality for a Reggeon contribution (in the Born approximation) and of Q^2 -independent intercepts for Pomeron and f -Reggeon trajectories. We compare these models using the above common set of experimental data.

3.1 Kinematics

We use the standard kinematic variables to describe deep inelastic scattering (DIS) :

$$e(k) + p(P) \rightarrow e(k') + X, \quad (3.1)$$

where k, k', P are the four-momenta of the incident electron, scattered electron and incident proton. Q^2 is the negative squared four-momentum transfer carried by the virtual exchanged photon (virtuality)

$$Q^2 = -q^2 = -(k - k')^2. \quad (3.2)$$

x is the Björken variable

$$x = \frac{Q^2}{2P \cdot q}, \quad (3.3)$$

³ In following Tables 2-7 the values of parameters and errors are presented in the form given by MINUIT, not rounded.

W is the center of mass energy of the (γ^*, p) system, related to the above variables by

$$W^2 = (q + P)^2 = Q^2 \frac{1-x}{x} + m_p^2, \quad (3.4)$$

with m_p being the proton mass.

3.2 Soft and Hard Pomeron models at small x .

3.2.1 Soft + Hard Pomeron (S+HP) model.

Considering the two-Pomeron model of Donnachie and Landshoff (D-L), we use a recently published variant [7]⁴ and write the proton SF as the sum of three Regge contributions: a hard and a soft Pomeron and an f -Reggeon

$$F_2(x, Q^2) = F_{hard} + F_{soft} + F_f, \quad (3.5)$$

where

$$F_{hard} = C_h \left(\frac{Q^2}{Q^2 + Q_h^2} \right)^{1+\epsilon_h} \left(1 + \frac{Q^2}{Q_h^2} \right)^{\frac{1}{2}\epsilon_h} \left(\frac{1}{x} \right)^{\epsilon_h}, \quad (3.6)$$

$$F_{soft} = C_s \left(\frac{Q^2}{Q^2 + Q_s^2} \right)^{1+\epsilon_s} \left(1 + \sqrt{\frac{Q^2}{Q_{s0}^2}} \right)^{-1} \left(\frac{1}{x} \right)^{\epsilon_s}, \quad (3.7)$$

$$F_f = C_f \left(\frac{Q^2}{Q^2 + Q_f^2} \right)^{\alpha_f(0)} \left(\frac{1}{x} \right)^{\alpha_f(0)-1} \quad (3.8)$$

with the cross-section (we approximate the total cross-section as the transverse one)

$$\sigma_T^{\gamma p}(W^2) = \frac{4\pi^2\alpha}{Q^2} F_2(x, Q^2) \Big|_{Q^2=0} = 4\pi^2\alpha \sum_{i=h,s,f} \frac{C_i}{(Q_i^2)^{1+\epsilon_i}} (W^2 - m_p^2)^{\epsilon_i}. \quad (3.9)$$

where $\epsilon_f = \alpha_f(0) - 1$.

We show in Table 2 results of the fit performed in the regions A₁ and B₁.

In order to take full advantage of the parametrization, but in contradiction with the original more economic suggestion of D-L, we allowed for the intercepts of the Soft Pomeron and f -Reggeon to be free.

In both regions, the values of Q_f^2 are found too small. If we put the low limit for this parameter at $0.076 \text{ GeV}^2 (\approx 4m_\pi^2)$, minimal physical threshold in t -channel), then $\chi^2/d.o.f.$ increases a little up to 1.192 in the fit A₁ and up to 1.283 in the fit B₁.

If the above mentioned 12 BCDMS and SLAC points are taken into account then we obtain

$$\begin{aligned} \chi^2/d.o.f. &= 1.097 && \text{in region A,} \\ \chi^2/d.o.f. &= 1.504 && \text{in region B} \end{aligned}$$

with free intercepts of Pomeron and f -Reggeon.

One can see that decreasing the minimal energy of the data set always leads to a deterioration of the fit.

⁴When the present paper was practically finished, an other variant [16] appeared with a slightly changed soft Pomeron term and additional factors $(1-x)^b$ in each term. We repeated our calculations for this new version however we failed to obtain $\chi^2/d.o.f. < 1.5$ even for region A₁ if the soft pomeron term (3.7) does not have square root factor.

Table 2: Parameters of the "Soft + Hard Pomerons" model [7] obtained from our fits in the regions A₁ and B₁

Parameter	Fit A ₁ ($W \geq 6$ GeV)		Fit B ₁ ($W \geq 3$ GeV)	
	value	\pm error	value	\pm error
C_h	.460299E-01	.139016E-02	.479219E-01	.334416E-02
ϵ_h	.435721E+00	.417590E-02	.431656E+00	.945276E-02
Q_h^2 (GeV ²)	.101656E+02	.253932E+00	.985373E+01	.479673E+00
C_s	.356527E+00	.353337E-02	.354170E+00	.777590E-02
ϵ_s	.891515E-01	.138958E-02	.900833E-01	.319777E-02
Q_s^2 (GeV ²)	.667118E+00	.779835E-02	.672313E+00	.213077E-01
Q_{s0}^2 (GeV ²)	.129234E+03	.143884E+02	.912972E+02	.227659E+02
C_f	.340843E-02	.282839E-03	.475168E-01	.118216E-01
$\alpha_f(0)$.572827E+00	.578989E-02	.602908E+00	.268310E-01
Q_f^2 (GeV ²)	.351976E-04	.487792E-05	.540418E-02	.228127E-02
$\chi^2/d.o.f.$	1.089		1.176	

3.2.2 Soft Dipole Pomeron (SDP) model

Defining the Dipole Pomeron model for DIS, we start from the expression connecting the transverse cross-section of γ^*p interaction to the proton structure function F_2 and the optical theorem for forward scattering amplitude ⁵

$$\sigma_T^{\gamma^*p} = 8\pi\Im m A(W^2, Q^2; t=0) = \frac{4\pi^2\alpha}{Q^2(1-x)}(1 + 4m_p^2x^2/Q^2)F_2(x, Q^2); \quad (3.10)$$

the longitudinal contribution to the total cross-section, $\sigma_L^{\gamma^*p} = 0$ is assumed. Though we consider in this Subsection only small x we give here the complete parameterization [8] valid also at large values of x ; it will be fully exploited in the next Section. The forward scattering at W far from the s -channel threshold $W_{th} = m_p$ is dominated by the Pomeron and the f -Reggeon

$$A(W^2, t=0; Q^2) = P(W^2, Q^2) + f(W^2, Q^2), \quad (3.11)$$

$$f(W^2, Q^2) = iG_f(Q^2)(-iW^2/m_p^2)^{\alpha_f(0)-1}(1-x)^{B_f}. \quad (3.12)$$

$$G_f(Q^2) = \frac{C_f}{(1 + Q^2/Q_f^2)^{D_f(Q^2)}}, \quad (3.13)$$

$$D_f(Q^2) = d_{f\infty} + \frac{d_{f0} - d_{f\infty}}{1 + Q^2/Q_{fd}^2}, \quad (3.14)$$

$$B_f(Q^2) = b_{f\infty} + \frac{b_{f0} - b_{f\infty}}{1 + Q^2/Q_{fb}^2}. \quad (3.15)$$

As for the Pomeron contribution, we take it in the two-component form

$$P(W^2, Q^2) = P_1 + P_2, \quad (3.16)$$

⁵ Note the 8π factor in the optical theorem non included in [8].

with

$$P_1 = iG_1(Q^2)\ell n(-iW^2/m_p^2)(1-x)^{B_1(Q^2)}, \quad (3.17)$$

$$P_2 = iG_2(Q^2)(1-x)^{B_2(Q^2)}, \quad (3.18)$$

where

$$G_i(Q^2) = \frac{C_i}{(1+Q^2/Q_i^2)^{D_i(Q^2)}}, \quad i = 1, 2, \quad (3.19)$$

$$D_i(Q^2) = d_{i\infty} + \frac{d_{i0} - d_{i\infty}}{1+Q^2/Q_{id}^2}, \quad i = 1, 2, \quad (3.20)$$

$$B_i(Q^2) = b_{i\infty} + \frac{b_{i0} - b_{i\infty}}{1+Q^2/Q_{ib}^2}, \quad i = 1, 2. \quad (3.21)$$

We would like to comment the above expressions, especially the powers D_i and B_i varying smoothly between constants when Q^2 goes from 0 to ∞ . In spite of an apparently cumbersome form they are a direct generalization of the exponents d and b appearing in each term of the simplest parametrization of the γ^*p -amplitude

$$G(Q^2) = \frac{C}{(1+Q^2/Q_0^2)^d} \quad \text{and} \quad (1-x)^b.$$

Indeed, a fit to experimental data shows unambiguously that the parameters d and b should depend on Q^2 .

At small $x \leq 0.07$, which are under interest now, it is not necessary to keep factors $(1-x)^{B_i}$, significant only when x gets near 1, in (3.12,3.17,3.18), with $B_i = B_i(Q^2)$. In order to exclude in the expression for F_2 (rather than for $\sigma_T^{\gamma^*p}$) any factors $(1-x)$, we should fix $B_i = -1$ in the above equations. In this case the S+HP and the SDP models can be compared for small x under similar conditions.

The results of fitting the data in the regions A_1 and B_1 are given in Table 3.

The intercept of f -Reggeon is then fixed at the value $\alpha_f(0) = 0.785$ obtained [23] from the fit to hadronic total cross-sections.

One can see from this table that the quality of the data description in the Soft Dipole Pomeron model is quite high. Furthermore, the values of the fitted parameters are close in both regions. Thus we claim a good stability of the model when the minimal energy W of the data set is varying.

Moreover, and to enforce this statement, we have investigated the ability of the SDP model to describe data in other kinematical regions namely with "small" $x \leq 0.1$ and $Q_{max}^2 = 3000$ Gev². Results follow

$$\begin{aligned} \chi^2/d.o.f. &= 0.978 & \text{if} & \quad W \geq 6 \text{ GeV}, \\ \chi^2/d.o.f. &= 1.014 & \text{if} & \quad W \geq 3 \text{ GeV}. \end{aligned}$$

Parameters are stable again and are not strongly modified from those in Table 3 for the regions A_1 and B_1 .

If BCDMS and SLAC points are included in the fits the following results are obtained for $x \leq 0.07$

$$\begin{aligned} \text{Region A:} & \quad \chi^2/d.o.f. = 0.936, \\ \text{Region B:} & \quad \chi^2/d.o.f. = 1.021. \end{aligned}$$

However, as already noted, some of the fitted parameters are not stable under transition from region A to region B (in the present case, mainly the parameters d_{i0} are concerned).

Table 3: Parameters fitted in the Soft Dipole Pomeron model [8] simplified in the small- x regions A_1 and B_1 .

Parameter	Fit A_1 ($W \geq 6$ GeV)		Fit B_1 ($W \geq 3$ GeV)	
	value	\pm error	value	\pm error
C_1 (GeV $^{-2}$)	.222698E-02	.494472E-05	.222972E-02	.474366E-05
Q_1^2 (GeV 2)	.860804E+01	.213165E-01	.823921E+01	.207764E-01
Q_{1d}^2 (GeV 2)	.126690E+01	.694433E-02	.123648E+01	.711041E-02
$d_{1\infty}$.124426E+01	.301742E-02	.124032E+01	.298242E-02
d_{10}	.986652E+01	.391815E-01	.941385E+01	.384359E-01
C_2 (GeV $^{-2}$)	-.893679E-02	.228570E-04	-.889722E-02	.228190E-04
Q_2^2 (GeV 2)	.198085E+02	.496695E-01	.189066E+02	.486844E-01
Q_{2d}^2 (GeV 2)	.947165E+00	.687587E-02	.105738E+01	.820888E-02
$d_{2\infty} - d_{1\infty}$ (fixed)	.000000E+00	.000000E+00	.000000E+00	.000000E+00
d_{20}	.132941E+02	.939077E-01	.109375E+02	.818441E-01
$\alpha_f(0)$ (fixed)	.785000E+00	.000000E+00	.785000E+00	.000000E+00
C_f (GeV $^{-2}$)	.294850E-01	.893680E-04	.293259E-01	.774985E-04
Q_f^2 (GeV 2)	.182986E+02	.985102E-01	.176838E+02	.958663E-01
Q_{fd}^2 (GeV 2)	.616179E+00	.495589E-02	.659804E+00	.541872E-02
$d_{f\infty}$.134520E+01	.401477E-02	.135104E+01	.410773E-02
d_{f0}	.404273E+02	.267141E+00	.357568E+02	.236524E+00
$\chi^2/d.o.f.$	0.911		0.948	

3.2.3 Modified two-Pomeron (Mod2P) model

We already noted elsewhere [21, 23, 38] a very interesting phenomenological fact which occurs for total cross-sections. If a constant term (or a contribution from a Regge pole with intercept one) is added to the ordinary "supercritical" Pomeron with $\alpha_P(0) = 1 + \epsilon$ (for example in the popular Donnachie-Landshoff model [20]) the fit to the available data leads to a very small value of $\epsilon \sim 0.001$ and to a negative sign of the new constant term. This is valid when pp and $\bar{p}p$ total cross-sections are considered as well as when all cross-sections, including $\sigma_{tot}^{\gamma p}$ and $\sigma_{tot}^{\gamma\gamma}$, are taken into account. Due to this small value of ϵ one can expand the factor $(-is/s_0)^\epsilon$, entering in the supercritical Pomeron, keeping only two first terms and obtain, in fact, the Dipole Pomeron model. We would like to emphasize that the resulting parameters in such a modified Donnachie-Landshoff model for total cross-sections are very close to those obtained in the Dipole Pomeron model.

It has been demonstrated above that SDP model for $F_2(x, Q^2)$, simplified for low x , describes well (even better than S+HP model does) DIS data in a wide region of Q^2 . A natural question arises : does such a situation remain possible for $\sigma_T^{\gamma^* p}$ or for the proton structure function at any Q^2 ? In what follows, we suggest a modification of the model defined by (3.5-3.8) and argue that answer on the above question is positive.

In fact, we consider the original S+HP model with $\epsilon_h = 0$ modifying only residues and

redefining the coupling constants ⁶ to have for the cross-section the expression

$$\sigma_T^{\gamma p}(W^2) = 4\pi^2\alpha \left\{ \frac{C_0}{\epsilon} + \frac{C_s}{\epsilon} \left(\frac{W^2}{m_p^2} - 1 \right)^\epsilon + C_f \left(\frac{W^2}{m_p^2} - 1 \right)^{\alpha_f(0)-1} \right\}. \quad (3.22)$$

ϵ is inserted in the denominators in order to avoid large values of C_0 and C_s when $\epsilon \ll 1$ (this case occurs in the fit).

Thus we write

$$F_2(x, Q^2) = F_0 + F_s + F_f \quad (3.23)$$

where

$$F_0 = \frac{C_0 Q_0^2}{\epsilon} \left(\frac{Q^2}{Q^2 + Q_0^2} \right) \left(1 + \frac{Q^2}{Q_{01}^2} \right)^{d_0}, \quad (3.24)$$

$$F_s = \frac{C_s Q_s^2}{\epsilon (m_p^2/Q_s^2)^\epsilon} \left(\frac{Q^2}{Q^2 + Q_s^2} \right)^{1+\epsilon} \left(1 + \frac{Q^2}{Q_{s1}^2} \right)^{d_s} \left(\frac{1}{x} \right)^\epsilon, \quad (3.25)$$

$$F_f = \frac{C_f Q_f^2}{(m_p^2/Q_f^2)^{\alpha_f(0)-1}} \left(\frac{Q^2}{Q^2 + Q_f^2} \right)^{\alpha_f(0)} \left(1 + \frac{Q^2}{Q_{f1}^2} \right)^{d_f} \left(\frac{1}{x} \right)^{\alpha_f(0)-1}. \quad (3.26)$$

The values of the free parameters and χ^2 are given in Table 4.

Table 4: Values of the fitted parameters in the Modified two-Pomeron model

Parameter	Fit A ₁ ($W \geq 6$ GeV)		Fit B ₁ ($W \geq 3$ GeV)	
	value	\pm error	value	\pm error
C_0 (GeV ⁻²)	-.192614E+00	.347649E-05	-.192597E+00	.341593E-05
Q_0^2 (GeV ²)	.103160E+01	.240636E-04	.103160E+01	.240085E-04
Q_{01}^2 (GeV ²)	.120880E+01	.991056E-04	.120742E+01	.986103E-04
d_0	.287793E+00	.479038E-05	.288178E+00	.477790E-05
C_s (GeV ⁻²)	.191862E+00	.345642E-05	.191835E+00	.339575E-05
ϵ (fixed)	.101300E-02	.000000E+00	.101300E-02	.000000E+00
Q_s^2 (GeV ²)	.980419E+00	.227654E-04	.980571E+00	.227169E-04
Q_{s1}^2 (GeV ²)	.101808E+01	.825788E-04	.101742E+01	.822231E-04
d_s	.287548E+00	.469776E-05	.287925E+00	.468653E-05
C_f (GeV ⁻²)	.230047E+01	.828553E-02	.233104E+01	.753061E-02
$\alpha_f(0)$ (fixed)	.789500E+00	.000000E+00	.789500E+00	.000000E+00
Q_f^2 (GeV ²)	.102321E+01	.622960E-02	.987669E+00	.571238E-02
Q_{f1}^2 (GeV ²)	.703071E+01	.128642E+00	.666517E+01	.119554E+00
d_f	.317443E+00	.130398E-02	.319035E+00	.128344E-02
$\chi^2/d.o.f.$	0.959		0.996	

One can see in Table 4 that $d_0 > d_s$ and that C_0 is negative. Consequently, at some high values of $Q^2 > Q_m^2(x)$, the SF (3.23) turns out to become negative. Numerically the minimal value of Q_m^2 where it occurs is *e.g.* $Q_m^2 \sim 4 \cdot 10^4$ GeV² at $x \sim 0.05$. It is far beyond the kinematical limit $y = \frac{Q^2}{x(s-m_p^2)} \leq 1$, with $s - m_p^2 \approx 4E_e E_p$, in terms of the positron E_e and

⁶We change also index "h" for "0" because now the term F_0 is no more a contribution of the hard Pomeron with high intercept.

proton E_p beam energies of an (ep) collider. For example, HERA measurements are presently restricted by $Q^2(\text{GeV}^2) \lesssim 10^5 x$. Besides this, at a so high virtuality, one-photon exchanges must be supplemented with other exchanges. On the other hand, from a phenomenological point of view, a fit respecting the condition $\delta = d_s - d_0 \geq 0$ yields the lower limit $\delta = 0$ and we obtained then $\chi^2/d.o.f. \approx 1.057$ in the region A_1 , better than in the S+HP model with a hard Pomeron. Finally, the result could be improved when replacing the constants d_i by functions $D_i(Q^2)$ such as (3.14), (3.20) in the SDP model. We do not consider this possibility in order to avoid an extra number of parameters.

For intercepts of Pomeron (ϵ) and of f -Reggeon ($\alpha_f(0)$), the values obtained in [23], in the case of non degenerated and non universal SCP are taken and fixed, in accordance with the idea of Reggeon universality (and because the data for $\sigma_{tot}^{\gamma p}$ are insufficient to determine precisely and simultaneously both the intercepts and the couplings).

For fits in the kinematical regions A and B (with BCDMS and SLAC points included) we have

$$\begin{aligned} \text{Region A:} \quad & \chi^2/d.o.f. = 0.963, \\ \text{Region B:} \quad & \chi^2/d.o.f. = 1.004. \end{aligned}$$

To complete the set of Regge models, we present now an other modification of the Donnachie and Landshoff model. At the same time, it can be considered as a generalization of the Soft Dipole Pomeron model.

3.2.4 Generalized logarithmic Pomeron (GLP) model.

We have found in [39] a shortcoming of the SDP model, relative to the logarithmic derivative $B_x = \partial \ln F_2(x, Q^2) / \partial \ln(1/x)$ at large Q^2 and small x . Namely, in spite of a good χ^2 in fitting the SF, theoretical curves for B_x are systematically lower than the data on this quantity extracted from F_2 . In our opinion, one reason might be a insufficiently fast growth of F_2 with x at large Q^2 and small x (the SDP model leads to a logarithmic behaviour in $1/x$). On the other side, essentially a faster growth of F_2 (and consequently of B_x) is, from a phenomenological point of view, a good feature of the D-L model. However, this model violates the known Froissart-Martin bound on the total cross-section of γ^*p process which, as commonly believed, should be valid at least for real photons.

Thus, we have tried to construct a model that incorporates a slow rise of $\sigma_T^{\gamma p}(W^2)$ and simultaneously a fast rise of $F_2(x, Q^2)$ at large Q^2 and small x . We propose below a model intended to link these desirable properties, being in a sense intermediate between the Soft Dipole Pomeron model (3.11)–(3.21) and the Modified two Pomeron (3.23)–(3.26) model. Again, as for SDP, we give a parameterization valid for all x , without restriction.

$$F_2(x, Q^2) = F_0 + F_s + F_f, \quad (3.27)$$

$$F_0 = C_0 \frac{Q^2}{(1 + Q^2/Q_0^2)^{d_0}} (1-x)^{B_0(Q^2)}, \quad (3.28)$$

$$F_s = C_s \frac{Q^2}{(1 + Q^2/Q_s^2)^{d_s}} L(Q^2, W^2) (1-x)^{B_s(Q^2)}, \quad (3.29)$$

where

$$L(Q^2, W^2) = \ln \left[1 + \frac{a}{(1 + Q^2/Q_{s0}^2)^{d_{s0}}} \left(\frac{Q^2}{xm_p^2} \right)^\epsilon \right] \quad (3.30)$$

$$F_f = C_f \frac{Q^2}{(1 + Q^2/Q_f^2)^{d_f}} \left(\frac{Q^2}{xm_p^2} \right)^{\alpha_f(0)-1} (1-x)^{B_f(Q^2)}, \quad (3.31)$$

where

$$B_i(Q^2) = b_{i\infty} + \frac{b_{i0} - b_{i\infty}}{1 + Q^2/Q_{ib}^2}, \quad i = 0, s, f. \quad (3.32)$$

A few comments on the above model are needed.

- In the original D-L model the dependence on x is in the form $(Q^2/x)^\epsilon$ but with $(Q^2)^\epsilon$ absorbed in a coupling function $(Q^2/(Q^2 + Q_s^2))^{1+\epsilon}$. The main modification (apart from a replacement of a power dependence by a logarithmic one) is that we inserted $(Q^2)^\epsilon$ into "energy" variable Q^2/x and made it dimensionless. By a similar way we modified the f -term.
- The new logarithmic factor in (3.29) can be rewritten in the form

$$L(Q^2, W^2) = \ell n \left[1 + \frac{a}{(1 + Q^2/Q_{s0}^2)^{d_{s0}}} \left(\frac{W^2 + Q^2}{m_p^2} - 1 \right)^\epsilon \right].$$

At $Q^2 = 0$, we have $L(0, W^2) = \ell n[1 + a(W^2/m_p^2 - 1)^\epsilon]$ and consequently $L(0, W^2) \approx \epsilon \ell n(W^2/m_p^2)$ at $W^2/m_p^2 \gg 1$. Thus, $\sigma_T^p(W) \propto \ell n W^2$ at $W^2 \gg m_p^2$. A similar behaviour can be seen at moderate Q^2 when the denominator is ~ 1 . However at not very large W^2/m_p^2 or at sufficient high Q^2 the argument of logarithm is close to 1, and then

$$L(Q^2, W^2) \approx \frac{a}{(1 + Q^2/Q_{s0}^2)^{d_{s0}}} \left(\frac{W^2}{m_p^2} - 1 \right)^\epsilon$$

simulating a Pomeron contribution with intercept $\alpha_P(0) = 1 + \epsilon$.

- We are going to justify that, in spite of its appearance, the GLP model cannot be treated as a model with a hard Pomeron, even when ϵ issued from the fit is not small. In fact, the power ϵ inside the logarithm is NOT the intercept (more exactly is not $\alpha_P(0) - 1$). Intercept is defined as position of singularity of the amplitude in j -plane at $t = 0$. In our case, the true leading Regge singularity is located exactly at $j = 1$: it is a double pole due to the logarithmic dependence. Let consider any fixed value of Q^2 and estimate the partial amplitude with the Mellin transformation

$$\begin{aligned} \phi(j, t = 0) &\sim \int_{W_{min}^2}^{\infty} dW^2 \left(\frac{W^2}{W_{min}^2} \right)^{-j} A(W^2, 0) \\ &\propto \int_{W_{min}^2}^{\infty} \frac{dW^2}{W^2} e^{-(j-1)\ell n(W^2/W_{min}^2)} \ell n \left(1 + a \frac{[(W^2+Q^2)/m_p^2 - 1]^\epsilon}{(1+Q^2/Q_0^2)^{d_{s0}}} \right). \end{aligned}$$

One can see that the singularities of $\phi(j, 0)$ are generated by a divergence of the integral at the upper limit. To extract them we can put the low limit large enough, say W_1^2 . The remaining integral, from W_{min}^2 to W_1^2 , will only contribute to the non-singular part of ϕ . We can take W_1^2 so large to allow the approximation $\ell n \left(1 + a \frac{[(W^2+Q^2)/m_p^2 - 1]^\epsilon}{(1+Q^2/Q_0^2)^{d_{s0}}} \right) \approx \epsilon \ell n(W^2/m_p^2)$. In this approximation

$$\phi(j, t = 0) \propto \int_{\zeta_1}^{\infty} d\zeta e^{-(j-1)\zeta} \zeta \approx \frac{1}{(j-1)^2} \quad \text{with} \quad \zeta_1 = \ell n(W_1^2/m_p^2).$$

- Thus this model can be considered as a Dipole Pomeron model. In order to distinguish between it and the Soft Dipole Pomeron model presented in Section 3.2.2, we call this model as Generalized Logarithmic Pomeron (GLP) model.

Performing fit in the regions A₁ and B₁, we fixed all $b_i = 0$, as required by the small x approximation, $\alpha_P(0)$ as in SDP, and obtained the results presented in Table 5.

Table 5: Values of the fitted parameters in the Generalized Logarithmic Pomeron model, simplified for low x

Parameter	Fit A ₁ ($W \geq 6$ GeV)		Fit B ₁ ($W \geq 3$ GeV)	
	value	\pm error	value	\pm error
C_0 (GeV ⁻²)	-.586790E+00	.590162E-02	-.622785E+00	.573266E-02
Q_0^2 (GeV ²)	.791206E+00	.121230E-01	.790649E+00	.113281E-01
d_0	.823491E+00	.264806E-02	.823973E+00	.251681E-02
C_s (GeV ⁻²)	.591058E+00	.341296E-02	.610089E+00	.334329E-02
a	.792225E+00	.912390E-02	.871875E+00	.935499E-02
ϵ	.331868E+00	.146863E-02	.318210E+00	.138877E-02
Q_{s0}^2 (GeV ²)	.566155E+00	.117036E-01	.512134E+00	.101668E-01
d_{s0}	.654811E+00	.276609E-02	.650015E+00	.260637E-02
Q_s^2 (GeV ²)	.447791E+00	.620657E-02	.458533E+00	.607371E-02
d_s	.541809E+00	.227447E-02	.532853E+00	.221010E-02
C_f (GeV ⁻²)	.201820E+01	.150381E-01	.198981E+01	.120945E-01
$\alpha_f(0)$ (fixed)	.785000E+00	.000000E+00	.785000E+00	.000000E+00
Q_f^2 (GeV ²)	.316038E+00	.566126E-02	.329387E+00	.551927E-02
d_f	.675356E+00	.369510E-02	.674280E+00	.361970E-02
$\chi^2/d.o.f.$	0.892		0.925	

In the "full" (i.e. with BCDMS and SLAC points) regions A and B the model gives

$$\text{Region A: } \chi^2/d.o.f. = 0.899,$$

$$\text{Region B: } \chi^2/d.o.f. = 0.948.$$

We complete, in the kinematical regions where $x \leq 0.1$

$$\chi^2/d.o.f. = 0.925 \quad \text{if} \quad W \geq 6 \text{ GeV},$$

$$\chi^2/d.o.f. = 0.955 \quad \text{if} \quad W \geq 3 \text{ GeV}.$$

3.2.5 Comparison between models at small x

Let us briefly discuss the obtained results when $x \leq 0.07$. In order to make the comparison between models more clear, we collect the corresponding $\chi_{d.o.f}^2$ -s in Table 6, where we recall also some characteristics of the models.

All investigated models well describe the data in the two kinematical regions. Nevertheless it is clear that the models without a hard Pomeron (the SDP model and especially the GLP one) are preferable to the original D-L model, which include a hard Pomeron with $\alpha_P(0) > 1$.

Table 6: Comparison of the quality of data descriptions at small x in the 4 investigated models; the kinematical regions are defined in the text

Model of Pomeron	Pomeron singularity	$\chi^2/d.o.f.$	
		Fit ($W > 6$ GeV) A ₁ ; A	Fit ($W > 3$ GeV) B ₁ ; B
Soft+Hard Pomeron (3.5)-(3.8)	simple poles	1.089	1.176
	$\alpha(0) > 1$	1.097	1.504
Soft Dipole Pomeron (3.11)-(3.21)	simple + double poles	0.911	0.948
	$\alpha(0) = 1$	0.936	1.021
Modified two-Pomeron (3.23)-(3.26)	simple poles	0.959	0.996
	$\alpha(0) \gtrsim 1, \alpha(0) = 1$	0.963	1.004
Generalized Logarithmic Pomeron (3.27)-(3.32)	simple + double poles	0.892	0.925
	$\alpha(0) = 1$	0.899	0.948

Thus in our opinion the most interesting and important result which has been derived from the above comparison of the models is that all SF data at $x < 0.1$ and $Q^2 \leq 3000$ GeV² are described with a high quality **without a hard Pomeron**. Moreover, these data support the idea that the soft Pomeron, either is a double pole with $\alpha_P(0) = 1$ in the angular momentum j -plane or is a simple pole having intercept $\alpha_P(0) = 1 + \epsilon$ with a very small ϵ . There is no contradiction with perturbative QCD where BFKL Pomeron has large ϵ . Firstly, it is well known that the corrections to BFKL Pomeron are large and the result of their summation is unknown yet. Secondly, the kinematical region ($x \ll 1$, $W^2 \gg Q^2$) is a region where the Regge approach should be valid and where non-perturbative contributions (rather than perturbative ones) probably dominate.

In fact, we have two soft Pomerons in the SDP and LGP models, the first one, simple pole located in j -plane exactly at $j = 1$ and giving a negative contribution to cross-section. This negative sign is a phenomenological fact, nevertheless such a term can be treated as a constant part of the dipole Pomeron rescatterings giving a negative correction to the single exchange. On the other hand a simple pole with intercept equal one can be treated as a crossing-even component three-gluon exchange [40].

The successful description of small- x domain within the SDP and GLP models allows us to apply them ⁷ to the extended region C, defined by the inequalities (2.3).

3.3 Soft Pomeron models at large x

In this section we present the results of the fits to the extended x -region, up to $x \leq 0.75$, *i.e.* to region C, performed in the Soft Dipole Pomeron model and in the newly proposed Generalized Logarithmic Pomeron model. The values of the fitted parameters, their errors as well as χ^2 are given in Table 7.

In order to compare the quality of our fits with those obtained in an other known model, we have performed as an example the same fit in the ALLM model [3]. This model incorporates an effective Pomeron intercept depending on Q^2 and cannot be considered as a Regge-type model. Nevertheless, it leads to a quite good description of the data in the same kinematical region: we obtained $\chi^2/d.o.f. \approx 1.11$ by limiting the intercept of f -Reggeon to a reasonable

⁷ We tried also to extend the Mod2P model to large x by using simple $(1-x)^{B_i(Q^2)}$ factors. We failed to get a good agreement with the data.

Table 7: Parameters obtained from the fit to the data set in region C ((2.3)) within the Soft Dipole Pomeron model (left) and the Generalized Logarithmic Pomeron model (right).

SDP model			GLP model		
Parameter	value	\pm error	Parameter	value	\pm error
C_1 (GeV ⁻²)	.210000E-02	.262020E-05	C_0 (GeV ⁻²)	-.860438E+00	.463009E-02
Q_1^2 (GeV ²)	.965340E+01	.126293E-01	Q_0^2 (GeV ²)	.133405E+01	.928886E-02
Q_{1d}^2 (GeV ²)	.154944E+01	.490752E-02	d_0	.113778E+01	.308424E-02
$d_{1\infty}$.130005E+01	.187044E-02	Q_{0b}^2 (GeV ²)	.741627E+01	.249967E+00
d_{10}	.866015E+01	.194363E-01	$b_{0\infty}$.703568E+01	.602611E-01
Q_{1b}^2 (GeV ²)	.315548E+00	.644633E-02	b_{00}	.142693E+01	.817529E-01
$b_{1\infty}$.290978E+01	.676692E-02			
b_{10}	-.205020E+02	.390882E+00			
C_2 (GeV ⁻²)	-.774241E-02	.819441E-05	C_s (GeV ⁻²)	.444070E+00	.200807E-02
Q_2^2 (GeV ²)	.219350E+02	.234796E-01	a	.143489E+01	.168555E-01
Q_{2d}^2 (GeV ²)	.300412E+01	.140016E-01	ϵ	.434764E+00	.166723E-02
$d_{2\infty} - d_{1\infty}$.000000E+00	.000000E+00	Q_{s0}^2 (GeV ²)	.188709E+00	.347041E-02
d_{20}	.433861E+01	.137719E-01	d_{s0}	.733135E+00	.281299E-02
Q_{2b}^2 (GeV ²)	.898304E+01	.871305E-01	Q_{s1}^2 (GeV ²)	.892069E+00	.915517E-02
$b_{2\infty}$.340630E+01	.455406E-02	d_s	.693609E+00	.267361E-02
b_{20}	.120264E+01	.150493E-01	Q_{sb}^2 (GeV ²)	.192698E+02	.135853E+01
			$b_{s\infty}$.110421E+02	.258010E+00
			b_{s0}	.312619E+01	.199118E+00
$\alpha_f(0)$ (fixed)	.785000E+00	.000000E+00	C_f (GeV ⁻²)	.211700E+01	.731039E-02
C_f (GeV ⁻²)	.277583E-01	.376481E-04	$\alpha_f(0)$ (fixed)	.785000E+00	.000000E+00
Q_f^2 (GeV ²)	.165653E+02	.238896E-01	Q_f^2 (GeV ²)	.901062E+00	.500511E-02
Q_{fd}^2 (GeV ²)	.384787E+00	.985244E-03	d_f	.863201E+00	.126160E-02
$d_{f\infty}$.136494E+01	.143903E-02	Q_{fb}^2 (GeV ²)	.280848E+01	.891465E-01
d_{f0}	.469211E+02	.111801E+00	$b_{f\infty}$.354614E+01	.826982E-02
Q_{fb}^2 (GeV ²)	.819589E+01	.809316E-01	b_{f0}	.832717E+00	.610819E-01
$b_{f\infty}$.332856E+01	.501372E-02			
b_{f0}	.680110E+00	.146980E-01			
$\chi^2/d.o.f.$	1.053		$\chi^2/d.o.f.$	1.074	

lower bound $\alpha_f(0) = 0.5$.

The behaviour of the theoretical curves for the cross-section $\sigma_{tot}^{\gamma p}$ versus the center of mass energy squared and for the proton structure function F_2 versus x for Q^2 ranging from the lowest to the highest values is shown in Figs. 1-4 for both models.

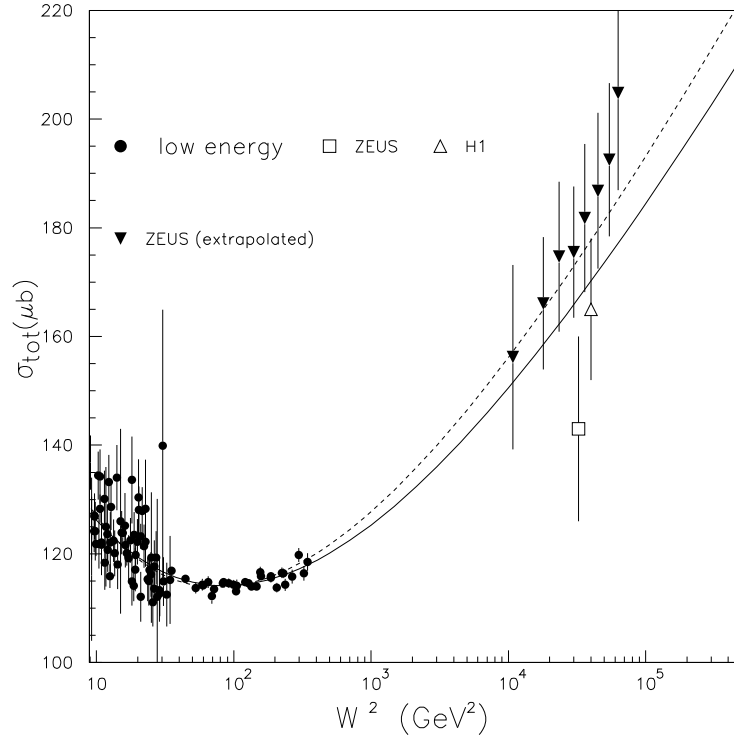


Figure 1: Total γp cross-section versus W^2 in SDP model (solid line) and in GLP model (dashed line). Data of [32] extracted from the SF at low Q^2 by the Zeus collaboration are also shown in the figure but not included in the fit.

One can see from the figures that

- both calculated γp cross-sections are above the two experimental HERA results at high energy; rather, they would be in agreement with the extrapolation performed [32] from very low Q^2 . The GLP model reveals a steeper rise with the energy than the SDP model.
- The calculated SDP and GLD proton structure functions can be distinguished by eye only outside the fitted range, especially at high Q^2 where the steeper rise of GLP model is evident.
- The SF curves calculated in the GLP model have a larger curvature (especially at high Q^2) than we expected and consequently larger logarithmic derivatives $B_x = \partial \ln F_2(x, Q^2) / \partial \ln(1/x)$ ⁸.

The last feature is reflected in the partial χ^2 for different intervals of Q^2 , as it can be seen in Table 8, where we compare the quality of the data description in such intervals. Indeed

⁸ A comparative detailed investigation of the derivatives of the proton structure with respect to x and Q^2 is under progress.

the GLP model "works" better in the region of intermediate Q^2 , while SDP model describes better the data at small and large Q^2 (including data on the total real γp cross-section). A similar analysis made for intervals in x would show that SDP model is more successful in region of small and large values of x and GLP model is for intermediate x , in agreement with the fact that the available data at intermediate Q^2 have also intermediate values of x .

Table 8: Partial values of χ^2 for different intervals of Q^2 in SDP and GLP models.

Interval of Q^2 (GeV ²)	Number of points	SDP model	GLP model
$Q^2=0$	99	121.96	133.15
$0 < Q^2 \leq 5$	404	325.30	348.32
$5 < Q^2 \leq 50$	540	621.81	614.73
$50 < Q^2 \leq 100$	101	112.47	94.27
$100 < Q^2 \leq 500$	150	141.79	151.62
$500 < Q^2 \leq 3000$	96	116.38	126.87

4 Conclusion

First of all, we would like to emphasize once more two important points.

1). The kinematical regions A (or A₁) and B (or B₁) where x is small are the domains where all conditions to apply the Regge formalism are satisfied : $W^2 \gg m_p^2$, $W^2 \gg Q^2$, $x \ll 1$. However because of universality of Reggeons and of existing correlations between Pomeron and f -Reggeon contributions, it is important to fix $\alpha_f(0)$ to the value determined from the hadronic data on resonances and on elastic scattering.

2). Analyzing the ability of any model to describe the data, it is necessary to verify how important are the assumptions on which the model is based. A possible mean holds in comparing the original model with an alternative one constructed without such assumptions (of course using a common set of experimental data).

In this work, we respect these two points and our conclusions are the following.

Small x . We have shown that the available data can be described without a hard Pomeron component. Moreover the models without a hard Pomeron lead to a better description of data (by $\approx 10\%$ in terms of χ^2). Furthermore, the best description is obtained in a model where the two Pomeron components have the trajectories with an intercept one.

We have proposed a new model for the proton structure function: the "Generalized Logarithmic Pomeron" model, which has not a hard Pomeron, but mimics its contribution at large Q^2 . In the region of small x this model gives the best $\chi^2/d.o.f$.

Small and large x . Multiplying each i -component of the Soft Dipole Pomeron and of the Generalized Logarithmic Pomeron models by a factor $(1-x)^{B_i(Q^2)}$, we can describe well not only small- x data but also data at all $x \leq 0.75$. As noted recently [16], these factors can be considered as an effective contribution of all daughter trajectories associated with Pomeron and f -Reggeon. Thus, their introduction is only an extension of the Regge approach to the whole kinematical x -region.

In spite of almost equivalent qualities of description, a precise analysis shows that these two models differently describe the data in the different regions of x and Q^2 . The extended

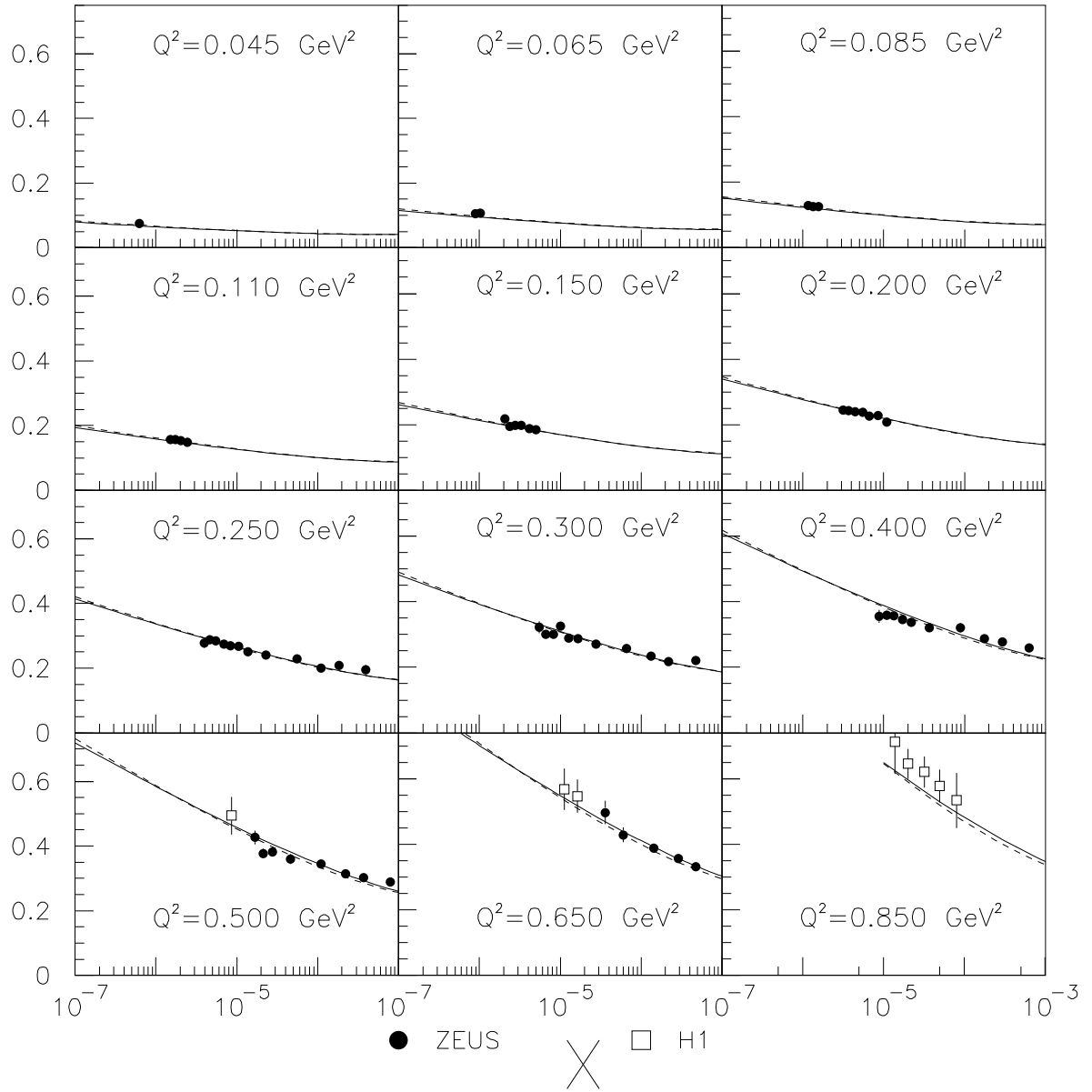


Figure 2: Structure function at small Q^2 versus x . Solid line is F_2 calculated within SDP model, dashed line is F_2 within GLP model.

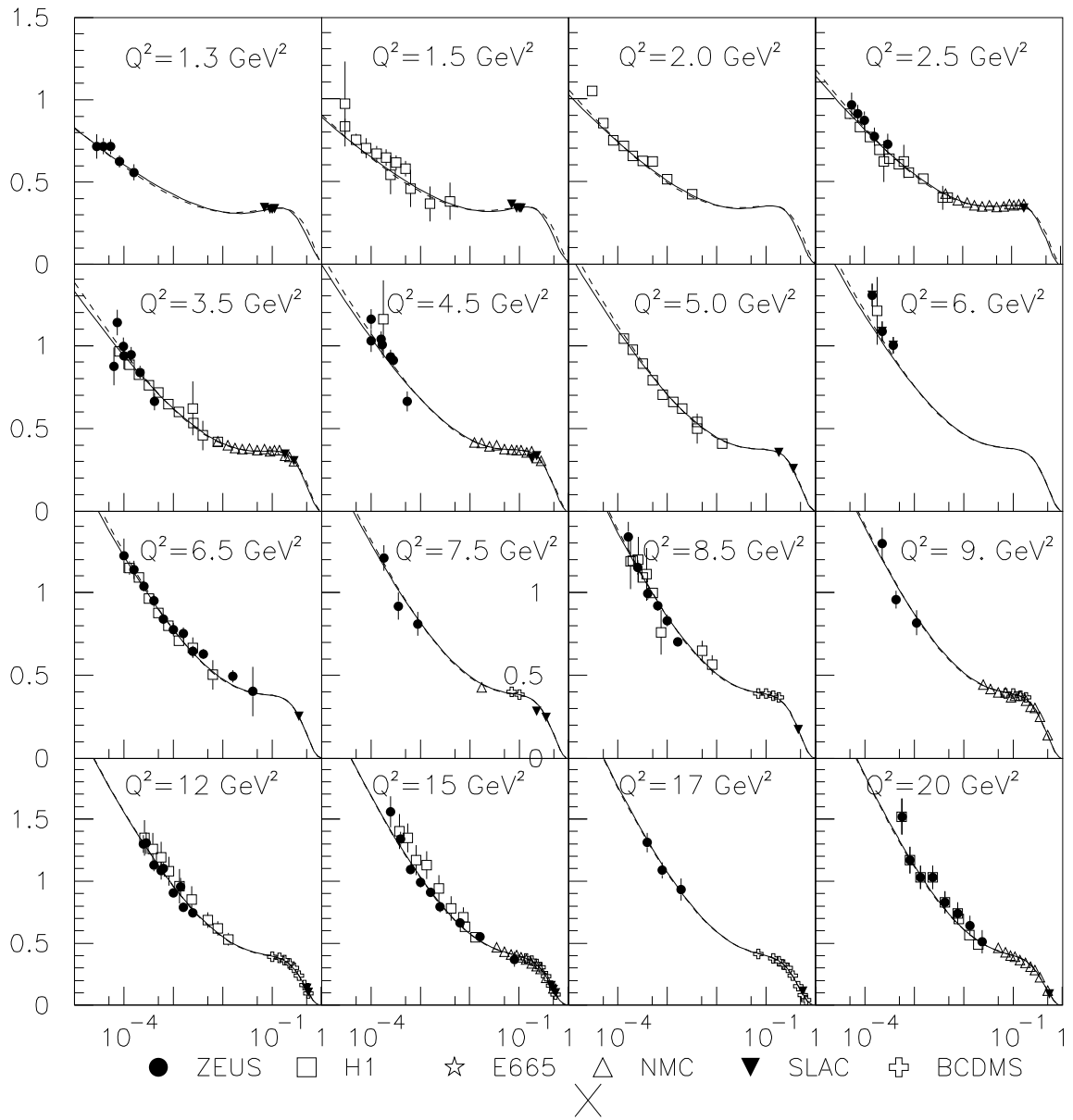


Figure 3: Same as in Fig. 2 for intermediate Q^2

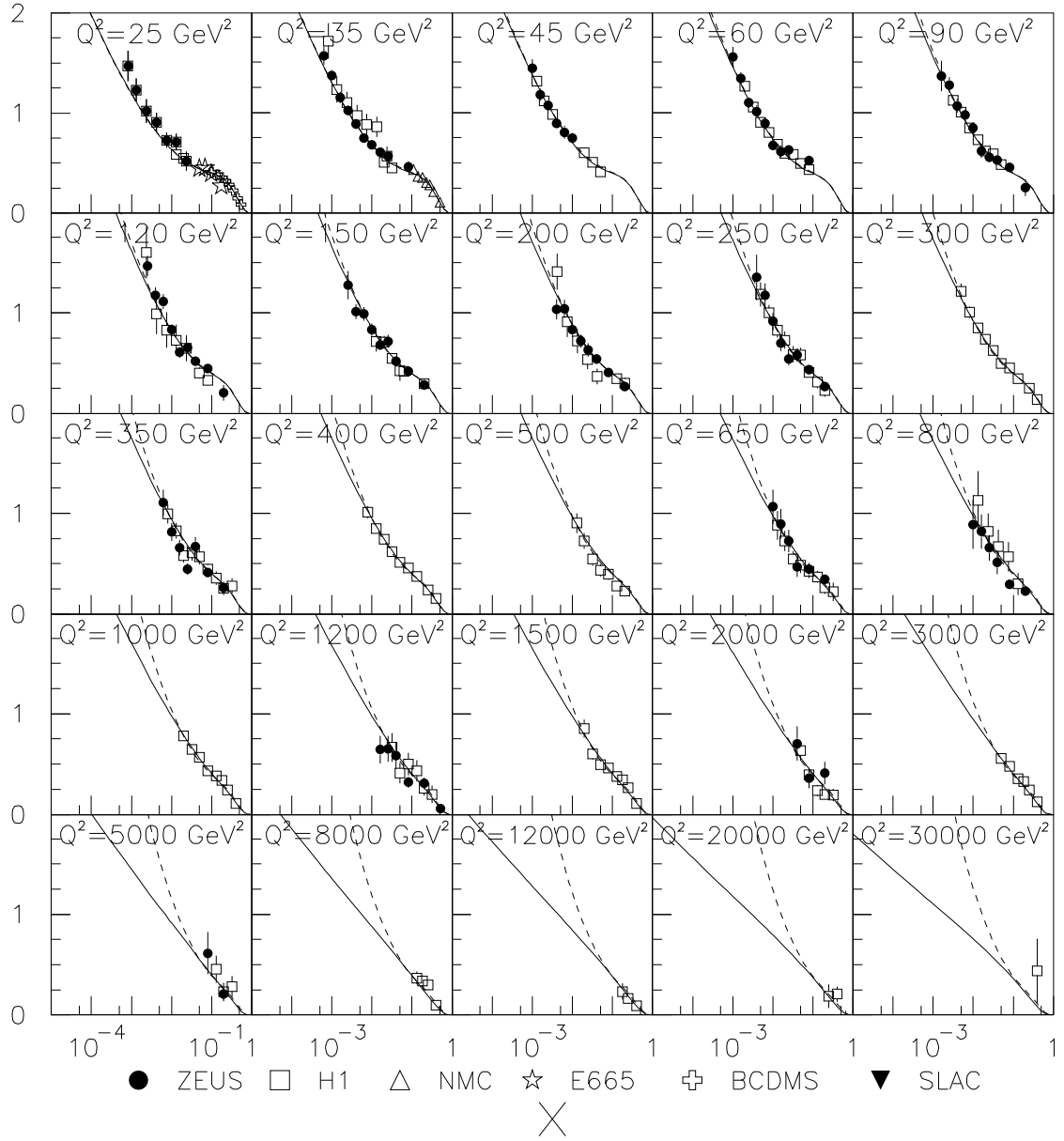


Figure 4: Same as in Fig. 2 for large Q^2 . The data represented in the lower row of icons, at $Q^2 \geq 5000 \text{ GeV}^2$, are not included in the fit

SDP model is more successful at small x , while the extended GLP model better describes the data at intermediate Q^2 and x . It would be interesting to construct a model incorporating the best features of both.

Concluding, we stress again that the available data on the proton structure function and on the γp cross-section do not yield explicit indications in favor of an existing hard Pomeron.

Acknowledgements We have the pleasure to thank M. Giffon for a critical reading of the manuscript.

References

- [1] P.D.B. Collins, *Introduction to Regge Theory and High Energy Physics*, Cambridge University Press (1977).
- [2] L.V. Gribov, E.M. Levin, M.G. Ryskin, Phys. Rep. **100**, 1 (1983).
- [3] H. Abramovicz *et al.*, Phys. Lett. B **269** 465, (1991);
H. Abramovicz, A. Levy, DESY 97-251, hep-ph/9712415 (1997).
- [4] B. Badelek, J. Kwiecinski, Phys. Lett. B **295**, 263 (1992); Rev. Mod. Phys. **68**, 445 (1996).
- [5] M. Bertini *et al.*, in "Strong interactions at long distances", edited by L. Jenkovszky, Hadronic Press, Palm Harbor, FL U.S.A, p.181, (1995).
- [6] A. Bialas, R. Peschanski, Ch. Royon, Phys. Rev. D **57** 6899 (1998).
- [7] A. Donnachie, P.V. Landshoff, Phys. Lett. B **437**, 408 (1998).
- [8] P. Desgrolard, S. Lengyel, E. Martynov, Eur. Phys. Jour. C **7**, 655 (1999); LYCEN 98102, hep-ph/9811380 (1998).
- [9] P. Desgrolard, L. Jenkovszky, F. Paccanoni, Eur. Phys. Jour. C **7**, 263 (1999).
- [10] P. Desgrolard, L. Jenkovszky, A. Lengyel, F. Paccanoni, Phys. Lett. B **459**, 265 (1999).
- [11] V.A. Petrov, A.V. Prokudin, hep-ph/9912248 (1999).
- [12] N.N. Nikolaev, J. Speth, V.R. Zoller, Phys. Lett. B **473**, 157 (2000).
- [13] A.B. Kaidalov, hep-ph/0103011 (2001) and references therein.
- [14] D. Schildknecht, Nucl. Phys. (Proc.Suppl.) B **99**, 121 (2001);
G. Cvetič, D. Schildknecht, B. Surrow, M. Tentyukov, hep-ph/0102229 (2001).
- [15] S.M. Troshin, N.E. Tyurin, hep-ph/0102322 (2001).
- [16] A. Donnachie, P.V. Landshoff, hep-ph/0105088 (2001).
- [17] H. Cheng, T.T. Wu, Phys. Rev. D **1**, 2775 (1970); Phys. Rev. Lett. **24**, 1456 (1970).

- [18] L.N. Lipatov, Sov. J. Nucl. Phys. **23**, 338 (1976); E.A. Kuraev, L.N. Lipatov, V.S. Fadin, Sov. Phys. JETP **45**, 199 (1977); Y.Y. Balitsky and L.N. Lipatov, Sov. J. Nucl. Phys. **28**, 822 (1978).
- [19] V.S. Fadin, L.N. Lipatov, Phys. Lett. B **429**, 127 (1998) and references therein.
- [20] A. Donnachie, P.V. Landshoff, Phys. Lett. B **296**, 227 (1992).
- [21] P. Desgrolard, M. Giffon, A. Lengyel, E. Martynov, Nuovo Cim. A **107**, 637 (1994).
- [22] J.R. Cudell et al., Phys. Rev. D **61**, 034019 (2000).
- [23] P. Desgrolard, M. Giffon, E. Martynov, E. Predazzi, Eur. Phys. J. C **18**, 555 (2001).
- [24] H1 collaboration, C. Adloff *et al.*, DESY-00-181, hep-ex/0012053 (2000).
- [25] ZEUS collaboration, J. Breitweg *et al.*, Nucl. Phys. B **487**, 53 (2000).
- [26] H1 collaboration, T. Ahmed *et al.*, Nucl. Phys. B **439**, 471 (1995).
- [27] H1 collaboration, S. Aid *et al.*, Nucl. Phys. B **470**, 3 (1996).
- [28] H1 collaboration, C. Adloff *et al.*, Nucl. Phys. B **497**, 3 (1997).
- [29] H1 collaboration, C. Adloff *et al.*, Eur. Phys. J. C **13**, 609 (2000).
- [30] ZEUS collaboration, M. Derrick *et al.*, Zeit. Phys. C **72**, 399 (1996).
- [31] ZEUS collaboration, J. Breitweg *et al.*, Phys. Lett. B **407**, 432 (1997).
- [32] ZEUS collaboration, J. Breitweg *et al.*, Eur. Phys. J. C **7**, 609 (1999).
- [33] NMC collaboration, M. Arneodo *et al.*, Nucl. Phys. B **483**, 3 (1997).
- [34] E665 collaboration, M.R. Adams *et al.*, Phys. Rev. D **54**, 3006 (1996).
- [35] L. W. Whitlow (Ph. D. thesis), SLAC-PUB 357 (1990);
SLAC old experiments, L. W. Whitlow *et al.*, Phys. Lett. B **282**, 475 (1992).
- [36] BCDMS collaboration, A. C. Benvenuti *et al.*, Phys. Lett. B **223**, 485 (1989).
- [37] The data on the total γp cross-section are extracted from <http://pdg.lbl.gov>.
ZEUS collaboration, M. Derrick *et al.*, Zeit. Phys. C **63**, 391 (1994);
H1 collaboration, S. Aid *et al.*, Zeit. Phys. C **69**, 27 (1995).
- [38] P. Desgrolard, M. Giffon, E. Martynov, E. Predazzi, Eur. Phys. J. C **9**, 623 (1999).
- [39] P. Desgrolard, A. Lengyel, E. Martynov, Nucl. Phys. (Proc. Suppl.) B **99**, 168 (2001).
- [40] L.N. Lipatov, Nucl. Phys. (Proc. Suppl.) B **79**, 207 (1999);
J. Bartels, L.N. Lipatov, G.P. Vacca, Phys. Lett. B **477**, 178 (2000).